Fermi National Accelerator Laboratory

FERMILAB-Conf-97/269-E
DØ

Jet Production at DØ

Victor Daniel Elvira
For the DØ Collaboration

SUNY at Stony Brook
Stony Brook, New York 11794

Fermi National Accelerator Laboratory
P.O. Box 500, Batavia, Illinois 60510

August 1997

Published Proceedings of *Les Rencontres de Physique de la Vallee d'Aoste*,
LaThuile, Italy, March 2-8, 1997

Disclaimer

Distribution

JET PRODUCTION AT DØ

Victor Daniel Elvira
for the DØ collaboration

SUNY at Stony Brook, Stony Brook, NY 11794, U.S.A.

Abstract

We report on preliminary measurements of the central ($|\eta| < 0.5$) inclusive jet cross section and the dijet angular distributions ($|\eta| < 3$) at $\sqrt{s} = 1.8$ TeV. The data were collected during the 1992–1993 and 1994–1995 runs at the Fermilab Tevatron $p\bar{p}$ Collider with the DØ detector. The measurements are in excellent agreement with next–to–leading order (NLO) QCD. Given the assumptions implicit in the theoretical models, we exclude quark compositeness to the 95% confidence level on a scale of Λ_+=2 TeV.

1 Introduction

High transverse momentum jets are predominantly produced in proton–antiproton collisions by two body scattering of a single proton constituent with an antiproton constituent. Predictions for the inclusive jet cross section [1, 2, 3] have been made using next–to–leading order (NLO) perturbative Quantum Chromodynamics (pQCD). These calculations to third order in the strong coupling constant (α_s^3) reduce theoretical uncertainties to $\approx 20\%$. We measure the cross section for the production of jets as a function of the jet energy transverse to the incident beams in the DØ detector [4] at the Fermilab Tevatron Collider. Previous measurements of inclusive jet production have been published by the UA2 [5] and CDF [6, 7] experiments. The CDF collaboration has reported excess jet production at large E_T relative to pQCD expectations [7].

Dijet final states in $p\bar{p}$ collisions can be produced through quark-quark, quark-gluon and gluon-gluon interactions. The angular distributions produced by these processes are similar, causing the dijet angular distributions to be fairly insensitive to uncertainties in the parton distribution functions (pdf's). The dijet angular distributions for QCD processes, which are mainly t-channel exchanges, are peaked at small center of mass scattering angles, while many processes containing new physics are more isotropic. These features make the dijet angular distributions an excellent test of perturbative QCD and a tool for searching for new physics such as quark compositeness. Data [8] previously submitted for publication, analyzed using a model with a left-handed contact interaction with destructive interference in which all quarks are composite, yield a 95% confidence limit $\Lambda_+ > 1.8$ TeV on the interaction scale.

2 Jet Detection

Jet detection in the DØ detector primarily requires the uranium–liquid argon calorimeters which cover pseudorapidity $|\eta| \leq 4.1$. Pseudorapidity is defined as $\eta = -\ln(\tan(\theta/2))$, where θ is the polar angle of the object relative to the proton beam. The calorimeter has trigger tiles of segmentation $\Delta\eta \times \Delta\phi = 0.8 \times 1.6$ and trigger towers of $\Delta\eta \times \Delta\phi = 0.2 \times 0.2$, where φ is the azimuthal angle. For $|\eta| \leq 0.5$ the calorimetric depth exceeds seven nuclear interactions lengths. The DØ detector includes two trigger scintillator hodoscopes located on each side of the interaction region. Timing distributions of particles traversing the two hodoscopes indicate the occurance of single or multiple $p\bar{p}$ collisions during a single beam–beam crossing. The event vertex is determined using tracks recon-

structed in the central tracking system.

Online event selection occurs in two hardware stages and a final software stage. The initial hardware trigger selected an inelastic particle collision as indicated by the hodoscopes. The next trigger stage required transverse energy above a preset threshold in the calorimeter trigger tiles for 1994–1995 data and towers for the 1992–1993 data. Selected events were digitized and sent to an array of processors. Jet candidates were then reconstructed with a fast cone algorithm and the entire event logged to tape if any jet E_T exceeded a specified threshold. During the 1994–1995 (1992–1993) data run, the software jet thresholds were 30, 50, 85, and 115 (20, 30, 50, 85, 115) GeV with total integrated luminosities for unprescaled triggers of 93 pb^{-1}(13 pb^{-1}), respectively.

3 Reconstruction and Offline Selection

Jets are reconstructed offline using an iterative jet cone algorithm with a cone radius of $\mathcal{R}$=0.7 in η–φ space [9]. Data are only used where the triggers are fully efficient. Background jets from isolated noisy calorimeter cells and accelerator losses are eliminated with quality cuts. Background events from cosmic ray bremsstrahlung are eliminated by requiring the missing E_T in an event to be less than 70% of the leading jet E_T. The efficiencies for these cuts are E_T and η dependent and are between 90-97%.

The dijet mass and kinematic variables of an event are defined using the two highest E_T jets. The center of mass scattering angle, θ^*, and the longitudinal boost, $\eta_{\rm boost}$, are expressed in terms of the pseudorapidities of these two jets: $\eta_{\rm boost}=\frac{1}{2}(\eta_1+\eta_2)$ and $\cos\theta^*=\tanh\eta^*$, where $\eta^*=\frac{1}{2}(\eta_1-\eta_2)$. The dominance of spin-1 gluon exchange gives the characteristic angular distribution of Rutherford scattering; $\mathrm{d}N/\mathrm{d}\cos\theta^* \propto (1-\cos\theta^*)^{-2}$. To facilitate an easier comparison with theory, the angular distribution is measured as a function of $\chi=e^{2|\eta^*|}$. For Rutherford scattering the $\mathrm{d}N/\mathrm{d}\chi$ spectrum is flat.

For the dijet angular distributions there is a dijet mass (M) threshold and restrictions on the kinematic cuts in order to limit the jets to regions of uniform acceptance [10]. The dijet mass is calculated by assuming each jet is massless; $M^2 = 2E_{T1}E_{T2}(\cosh(\eta_1-\eta_2)-\cos(\varphi_1-\varphi_2))$. Both $|\eta_1|$ and $|\eta_2|$ are required to be less than 3.0. To maintain uniform acceptance, we also require $|\eta_{\rm boost}| < 1.5$.

4 Energy Corrections

The jet energy calibration is performed in a multi-step process [11]. First, the electromagnetic energy scale in the central calorimeter is determined by scaling the energies of electrons from Z° decays so that the corrected Z° mass agrees with the value measured at LEP [12]. Next, the response versus jet energy in the central calorimeter is measured from photon + jet events, using transverse momentum conservation. After determining the jet response in the central calorimeter, the relative η dependent jet response is measured using both photon + jet and dijet events. One jet (photon) is required to be central and the jet response is measured as a function of the η of the probe jet. Jets are also corrected for out-of-cone showering losses, underlying event, multiple $p\bar{p}$ interactions, and effects of noise. The jet energy scale correction was re–evaluated during 1996 with a significant reduction in the systematic uncertainty with respect to previously reported results [13]. At 100 GeV (400 GeV) the error was reduced from 3% (5%) to 2% (2.6%).

The steeply falling jet spectrum is distorted by jet energy resolution. At all E_T the resolution, as measured with dijet E_T balance, is well described by a gaussian distribution. The fractional resolution σ_{E_T}/E_T is 7% at 100 GeV. This number includes the correction for additional soft radiation and smearing caused by particles radiated outside the reconstruction cone. The observed inclusive jet E_T spectrum is corrected for resolution smearing by assuming a trial unsmeared spectrum $(A{E_T}^{-B}) \cdot (1 - 2E_T/\sqrt{s})^C$, smearing it with the measured resolution, and comparing the smeared result with the measured cross section. This procedure is repeated until the observed cross section and smeared trial spectrum are in good agreement. The correction reduces the observed cross section by 16$\pm$5% (8$\pm$5%) at 60 GeV (400 GeV).

In the case of the dijet angular distributions the energy and η resolution smearing effect is small and is included in the uncertainty.

5 Results

5.1 Inclusive Jet Cross Section

The fully corrected cross section for jets of $|\eta| \leq 0.5$ is shown in Figure 1. The error bars are statistical only. The inset shows the total systematic error (excluding the luminosity error) as a function of E_T. Figure 1 also shows a theoretical prediction for the cross section from the NLO event generator JETRAD [1]. Note the excellent agreement over

seven orders of magnitude. The data and theoretical calculations are binned identically in E_T. The NLO calculation requires specification of the renormalization and factorization scale, (we choose $\mu = E_T/2$ where E_T is the maximum jet E_T in the generated event), parton distribution function (pdf = CTEQ3M [14]), and the parton clustering algorithm. The CTEQ3M pdf includes the deep inelastic and recent HERA data as well as W boson asymmetry and Drell–Yan measurements.

Figure 2 shows the ratio, $(D - T)/T$, for the data (D) and NLO theoretical (T) predictions based on the CTEQ3M. The 1992–1993 and 1994–1995 data are in excellent agreement with each other and the theoretical prediction.

5.2 Dijet Angular Distributions

Figure 3 shows the dijet angular distributions compared to a LO and a NLO pQCD prediction using the JETRAD program [1]. Both predictions are for a single choice of renormalization/factorization scale, μ=E_T. Figure 3 also shows the dijet angular distributions compared to NLO JETRAD calculations for two different renormalization scales. The NLO predictions are in better agreement with the data than the LO calculations and the effects of the renormalization scale at NLO are significant. The pdf used in the theory calculation was CTEQ3M. We tried another pdf, CTEQ2MS [15], and the angular distributions were insensitive to the change.

The main systematic uncertainty on the angular distributions comes from the η dependent energy scale correction, which is found to be less than 2%. Other systematic errors, which include η biases in jet reconstruction, multiple $p\bar{p}$ interactions, η dependent jet quality cut efficiencies, and effects of calorimeter η and E_T smearing are small. Since we present distributions normalized to the total number of events, the uncertainties from the absolute jet energy scale are minimal. All errors are added in quadrature to obtain the total systematic error which is shown as a band at the bottom of Figures 3– 4.

Since the currently available NLO calculations do not implement the effects of quark compositeness, possible effects of quark compositeness are determined using PAPAGENO [16], a LO simulation. The ratio of the LO predictions with a compositeness model containing left-handed destructive contact interference with all quarks composite to the LO predictions with no compositeness is used to scale the NLO calculations. Figure 4 shows the dijet angular distribution for events with $M > 635$ GeV/c^2 compared to theory for different values of the compositeness scale, Λ_+. The largest dijet mass bin is shown because the effects of quark compositeness become more pronounced with increasing dijet

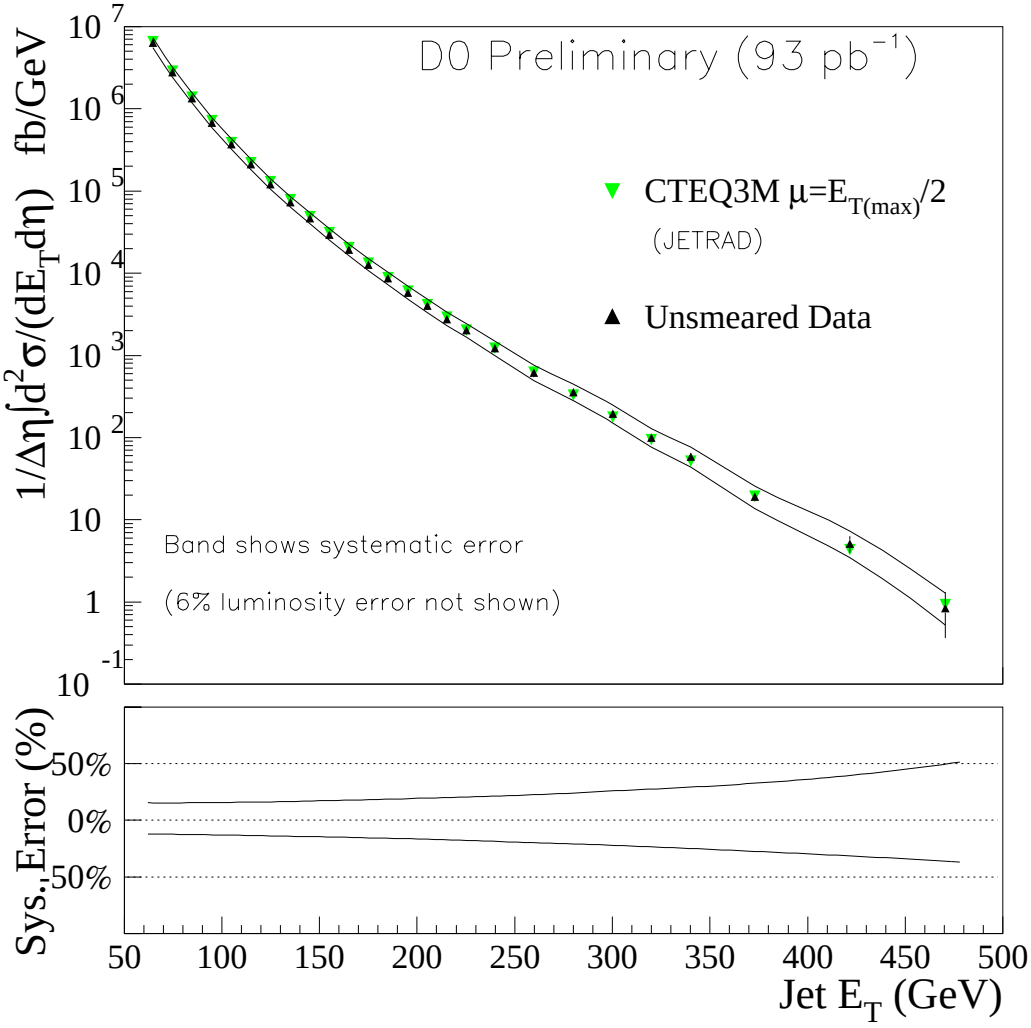

Figure 1: A comparison of the central, $|\eta| \leq 0.5$, inclusive cross section to a NLO calculation. The points include statistical errors. The inset curves represent plus and minus 1σ systematic error.

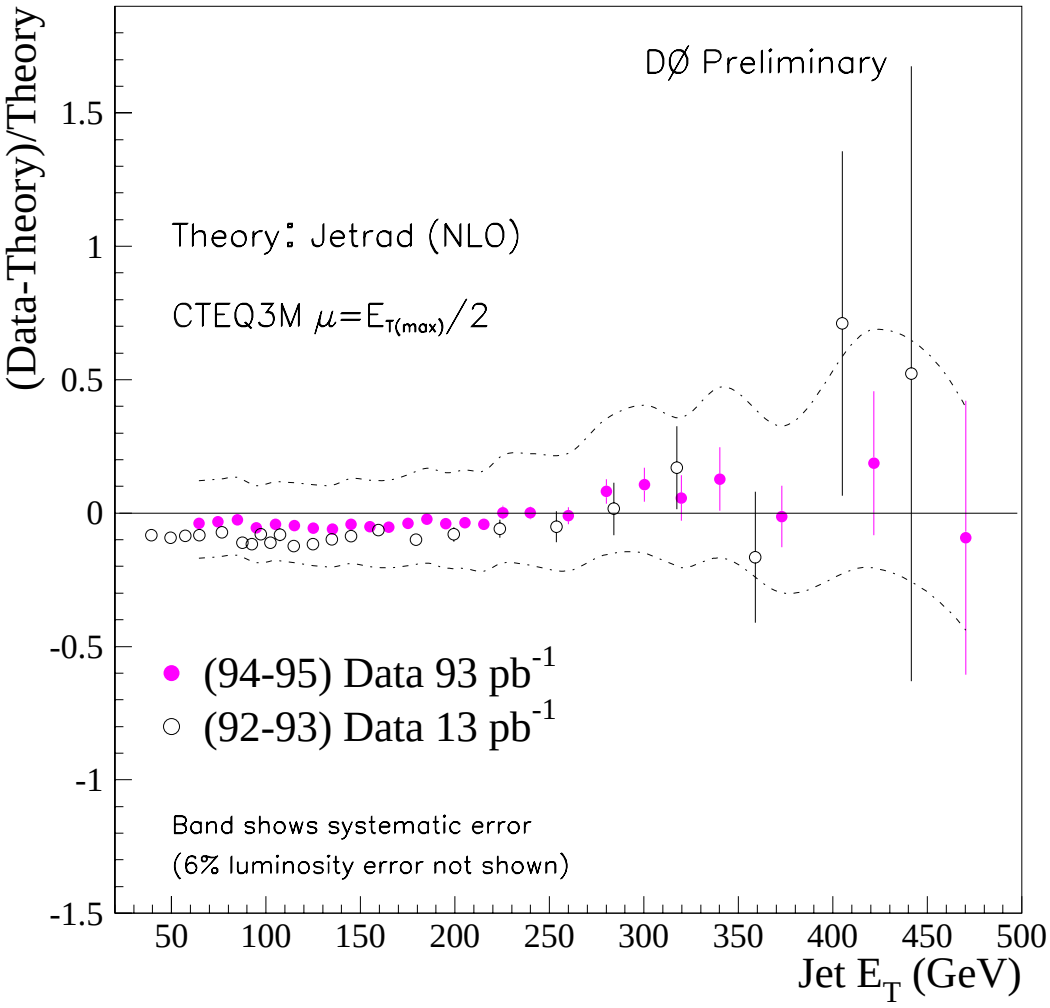

Figure 2: Difference between the data and pQCD predictions $((D-T)/T)$.

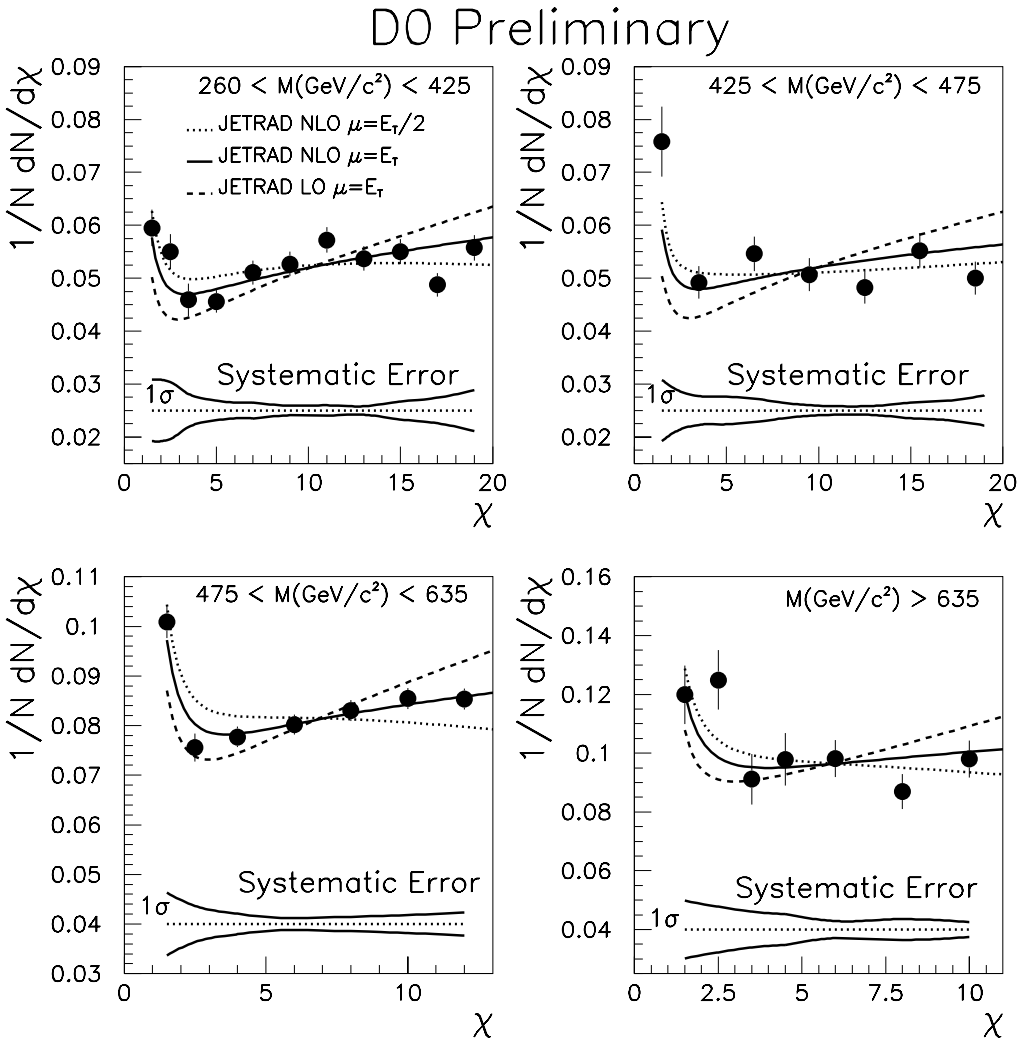

Figure 3: Dijet angular distributions for DØ data (circles) compared to JETRAD for LO and NLO predictions with renormalization scale μ=E_T. The data are also compared to JETRAD NLO predictions for two different renormalization scales. The errors on the data points are statistical. The band at the bottom represents the correlated $\pm$ 1 σ systematic error.

Table 1: The 95% confidence limits for the compositeness scale for different models. The prior probability distribution was assumed to be either flat in $1/\Lambda_+^2$ or $1/\Lambda_+^4$.

μ	Prior Dist.	Limit on Λ_+
$E_T/2$	$1/\Lambda_+^2$	2.2
E_T	$1/\Lambda_+^2$	2.0
$2E_T$	$1/\Lambda_+^2$	1.9
$E_T/2$	$1/\Lambda_+^4$	2.0

mass.

In order to obtain a compositeness limit, we constructed the variable R_χ, which is the ratio of the number of events with $\chi < 4$ to the number of events between $4 < \chi < \chi_{\rm max}$. The angular distribution of jets arising from a contact interaction will be more isotropic than pQCD and will produce more events at small values of χ, and therefore will have a larger value of R_χ.

We employed Bayesian techniques to obtain a compositeness scale limit from our data, using a Gaussian likelihood function, $P(R_\chi|\gamma)$, for R_χ as a function of dijet mass. The compositeness limit depends on the renormalization scale and the choice of the prior probability distribution, $P(\gamma)$, which was assumed to be either flat in $\gamma{=}1/\Lambda_+^2$ or $\gamma{=}1/\Lambda_+^4$.

Table 1 shows the 95% confidence limits for the compositeness scale obtained for the different choices of models.

6 Conclusions

We have done a preliminary measurement of the inclusive jet cross section for $|\eta| \leq 0.5$ and 35 GeV $\leq E_T \leq$ 470 GeV. NLO pQCD predictions are in excellent agreement with the observed central inclusive cross section. The dijet angular distribution was measured

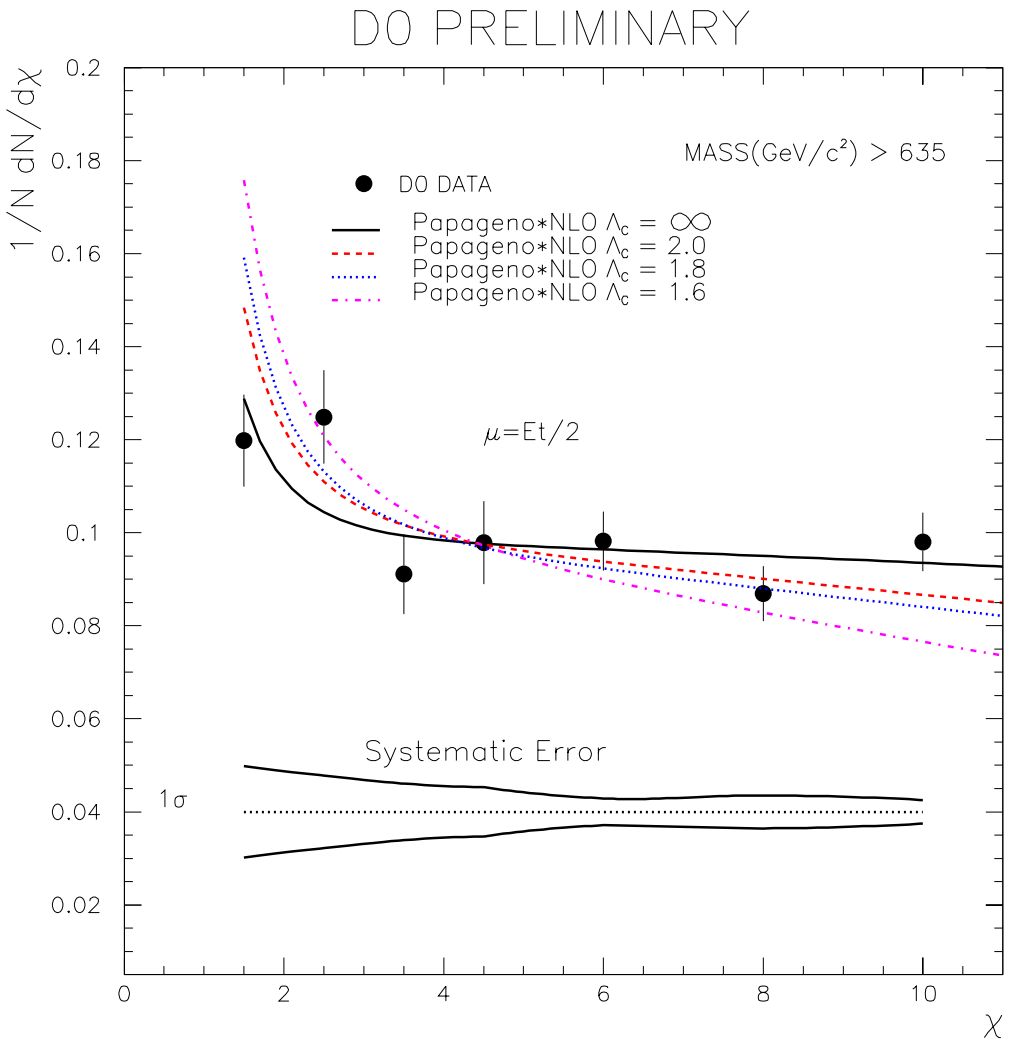

Figure 4: Data compared to theory for different compositeness scales. See text for how compositeness is calculated for NLO predictions. The errors on the points are statistical and the band represents the correlated $\pm$ 1 σ systematic error.

with greater precision over a larger dijet invariant mass range and a larger angular range than previous measurements. Our data distributions are in excellent agreement with NLO pQCD predictions. The compositeness limit depends upon the choice of both renormalization scale and the choice of the prior probability function. We have presented a compositeness limit for a model with a left-handed destructive contact interference with all quarks composite. With 95% confidence, the interaction scale, Λ_+, for this model exceeds approximately 2 TeV.

Acknowledgments

We thank W. Giele, E. Glover, and D. Kosower for their helpful comments and suggestions. We thank the staffs at Fermilab and collaborating institutions for their contributions to this work, and acknowledge support from the Department of Energy and National Science Foundation (U.S.A.), Commissariat à L'Energie Atomique (France), State Committee for Science and Technology and Ministry for Atomic Energy (Russia), CNPq (Brazil), Departments of Atomic Energy and Science and Education (India), Colciencias (Colombia), CONACyT (Mexico), Ministry of Education and KOSEF (Korea), CONICET and UBACyT (Argentina), and the A.P. Sloan Foundation.

References

[1] W. T. Giele, E. W. N. Glover, and D. A. Kosower, *Phys. Rev. Lett.* **73**, 2019 (1994).

[2] S. D. Ellis, Z. Kunszt, and D. E. Soper, *Phys. Rev. Lett.* **64**, 2121 (1990).

[3] F. Aversa, *et al.* , Journal*Phys. Rev. Lett.*651990.

[4] S. Abachi *et al.* (DØ Collaboration), *Nucl. Instrum. Methods* **A338**, 185 (1994).

[5] J. Alitti *et al.* (UA2 Collaboration), *Phys. Lett.* B **257**, 232 (1991); *Z. Phys.* C **49**, 17 (1991).

[6] F. Abe *et al.* (CDF Collaboration), *Phys. Rev. Lett.* **70**, 1376 (1993).

[7] F. Abe *et al.* (CDF Collaboration), *Phys. Rev. Lett.* **77**, 438 (1996).

[8] F. Abe *et al.* (CDF Collaboration), submitted to Phys. Rev. Lett.

[9] S. Abachi *et al.* (DØ Collaboration), *Phys. Lett.* B **357**, 500 (1995).

[10] Mary K. Fatyga, Ph.D. Thesis, University of Rochester, 1996 (unpublished).

[11] R. Kehoe, To appear in Proceedings of the VI$^{\text{th}}$ International Conference on Calorimetry in High Energy Physics, Laboratori Nazionali di Frascati Frascati, Italy (1996)

[12] P. Renton, Lepton-Photon Conference, Beijing, China (1995) OUNP-95-20.

[13] G. Blazey, presented at 31st Rencontres de Moriond: QCD and High-energy Hadronic Interactions, Les Arcs, France, 23-30 Mar 1996. In "Les Arcs 1996, QCD and high energy hadronic interactions", 155-164.

[14] H.L.Lai *et al.*, *Phys. Rev.* D **51**, 4763 (1995).

[15] J. Botts *et al.* (CTEQ Collaboration) Phys. Lett. B**304**, 159 (1993).

[16] I. Hinchliffe, LBL-34372, July, 1993.